SCIENTIFIC REPORTS

OPEN

SUBJECT AREAS:
SINGLE-MOLECULE BIOPHYSICS
MAGNETIC TWEEZERS
BIOPHYSICAL CHEMISTRY
BIOLOGICAL PHYSICS

Received
25 April 2013

Accepted
29 November 2013

Published
16 December 2013

Correspondence and requests for materials should be addressed to J.Y. (phyyj@nus.edu.sg)

Mechanosensing of DNA bending in a single specific protein-DNA complex

Shimin Le[1,2], Hu Chen[1,3], Peiwen Cong[1,4], Jie Lin[1,3], Peter Dröge[5] & Jie Yan[1,2,3]

[1]Mechanobiology Institute, National University of Singapore, Singapore, 117411, [2]Centre for Bioimaging Sciences, National University of Singapore, Singapore, 117546, [3]Department of Physics, National University of Singapore, Singapore, 117542, [4]Singapore-MIT Alliance, National University of Singapore, Singapore, 117542, [5]Division of Molecular Genetics and Cell Biology, School of Biological Sciences, Nanyang Technological University, Singapore, 637551.

Many crucial biological processes are regulated by mechanical stimuli. Here, we report new findings that pico-Newton forces can drastically affect the stability of the site-specific DNA binding of a single transcription factor, the *E. coli* integration host factor (IHF), by stretching a short ~150 nm DNA containing a single IHF binding site. Dynamic binding and unbinding of single IHF were recorded and analyzed for the force-dependent stability of the IHF-DNA complex. Our results demonstrate that the IHF-DNA interaction is fine tuned by force in different salt concentration and temperature over physiological ranges, indicating that, besides other physiological factors, force may play equally important role in transcription regulation. These findings have broad implications with regard to general mechanosensitivity of site-specific DNA bending proteins.

Site-specific DNA binding by proteins is a crucial process for gene transcription and its regulation. For example, RNA polymerase binds to specific promoter sequences to initiate transcription, while many DNA-binding transcription factors also bind to these sequences in order to regulate the level of the transcription[1]. In eubacteria, e.g. *E. coli*, there are approximately 400 DNA-binding transcription factors[1,2]. Site-specific binding is also essential to many other DNA transactions, such as site-specific recombination and replication[3–5]. Therefore, detailed knowledge of DNA binding properties of site-specific proteins will provide important insights to their regulatory functions.

It has been known that the activities of many site-specific DNA binding proteins are regulated by various environmental factors, such as temperature, salt osmolarity, pH value, as well as other cellular proteins. While the sensitivities of site-specific DNA binding to these factors have been extensively studied by various experimental approaches, the potential role of force has been much less investigated.

Only very recently the mechanical force has been recognized as an important physiological factor that plays critical functions in diverse biological processes. *In vivo*, forces are produced by various cellular machineries. For example, in nucleus, individual DNA and RNA polymerases can exert up to ~30 pN on DNA during actions[6,7]. Due to the ubiquitous presence of forces on chromosomal DNA, force may potentially influence site-specific DNA binding by proteins. In this work, we seek to probe the site-specific DNA-protein interaction on a single-DNA tether placed under force. As many DNA binding transcription factors cause DNA bending upon binding, the model system we chose is the *E. coli* integration host factor (IHF); a well-known DNA bending protein which binds to several specific sequences.

IHF was originally discovered as an essential co-factor for site-specific recombination of phage λ into *E. coli* genome[3]. It also regulates various gene transcriptions in *E. coli*[8] and *S. typhimurium*[9]. Various functions of IHF rely largely on its site-specific binding[1,10]. Among several specific sequences to which IHF binds with high affinity[4], the ~34 bp H′ sequence in the bacteriophage λ attachment site has the strongest binding affinity to IHF. Its dissociation constant is in the range of 2–20 nM[4] according to previous bulk biochemistry measurements, and <1 nM according to a recent stop flow measurement[11]. The IHF induced bending angle of H′ was determined to be ~160° by X-ray crystallization[5], >120° by atomic force microscopy (AFM) imaging[12–14].

Besides site-specific binding, as an abundant nucleoid-associated protein (NAP) with an intracellular concentration of 12–55 μM[15], IHF also associates with DNA non-specifically[16,17]. It is reported that in the presence of $MgCl_2$ in mM range, at high enough concentration, non-specific binding of IHF can mediate condensation of large DNA[16], suggesting a role of non-specific binding in packaging and shaping the genome.

Binding of IHF to specific sequences such as H′ sequence has been investigated by electrophoretic mobility shift assays (EMSAs) and footprinting[4,18], fluorescence resonance energy transfer (FRET)[19,20], isothermal titration

calorimetry (ITC)[17], stop-flow fluorimetry[11], tethered particle motion[21], and temperature jump[22]. IHF is able to bind to specific DNA sequences in both specific and non-specific modes. While non-specific binding may occur at high protein concentrations and low KCl concentration, specific binding dominates at low protein concentration or high KCl concentration[17]. In addition, several intermediate conformational states have been suggested by recent stop-flow fluorimetry[11] and time-resolved FRET[19].

However, in these studies DNA was not subject to force; therefore the potential role of force on specific IHF-H′ interaction remains unclear. To address how force may regulate the interaction between IHF and H′ sequence, here, we investigated the force-dependent stability of the conformational states of a single IHF-H′ complex in different salt, temperature and IHF concentration conditions. In addition, we also determined the bending angle of H′ induced by IHF in solution.

Results

Our study was based on DNA extension changes under tension induced by the docking of a single IHF protein to an H′ sequence inserted to the middle of a 445 bp (~150 nm in contour length) DNA that does not contain any other high-affinity site based on the known consensus sequence for IHF (SM-Text "DNA constructs") (Fig. 1a). The extension change was measured by magnetic tweezers with a spatial resolution of ~2 nm and a sampling rate of 100 Hz[23]. To ensure the specificity of the binding, parallel experiments were performed on a control DNA of the same sequence but lacking the H′ site (SM-Text "DNA constructs"). In *E. coli*, the $MgCl_2$ concentration is tightly regulated in a narrow range of 1–4 mM[24]. Therefore, in all our experiments of the specific interaction between IHF and H′ DNA sequence, 2.5 mM $MgCl_2$ was included to mimic the physiological condition.

Fig. 1b shows representative time traces recorded in 10 nM IHF, 50 mM KCl, 2.5 mM $MgCl_2$, 10 mM Tris (pH 7.4), and 21 ± 1°C at force range from 0.5–1 pN. Clear two-state fluctuations between a shorter DNA extension (bent DNA) and a longer DNA extension (unbent DNA) were observed. The two-state fluctuations were filtered with fast Fourier transformation, followed by two-state digitizing using a noise-beating step-finding algorithm similar to that developed by Cui et al[25]. (red data in Fig. 1b) (see details in supplementary materials). Such two-state fluctuations were not seen before IHF was introduced (Fig. S1). It was also absent with the control DNA construct of the same sequence but lacking the H′ site in the presence of IHF (Fig. S2). In addition, the force extension curves of a 48,502 bp long λ-DNA in the presence of 10 nM IHF were indistinguishable from that of the naked λ -DNA in 50 mM KCl (Fig. S3a), which suggested that non-specific binding of IHF does not play an observable role in this condition (note that on lambda DNA there are four high affinity consensus sites[26], but their contributions to the force-extension curves of the vast lambda DNA is negligible[27]). Thus, we conclude that the two-state fluctuation was both IHF and H′ sequence dependent.

Fig. 1c shows the normalized histogram of DNA extension distributions, which are apparently bimodal with two extension species, fitted with double Gaussian distributions at different forces (Fig. 1c). The distance between the two peaks calculated based on 40 such distributions is 17.34 ± 0.08 nm (mean ± s.d.) represented the extension difference of the two conformational states at the force range. Remarkably, a small force change of sub-pN switched the lower extension state from more probable to less probable, suggesting that the balance between the two states can be fine-tuned by adjusting force over a narrow range.

The force-dependent probability of the bent DNA state, P_{bent}, can be calculated by the relative area of the two species in the bimodal extension distribution. This probability is related to the free energy difference between the two states through the Boltzmann distribution:

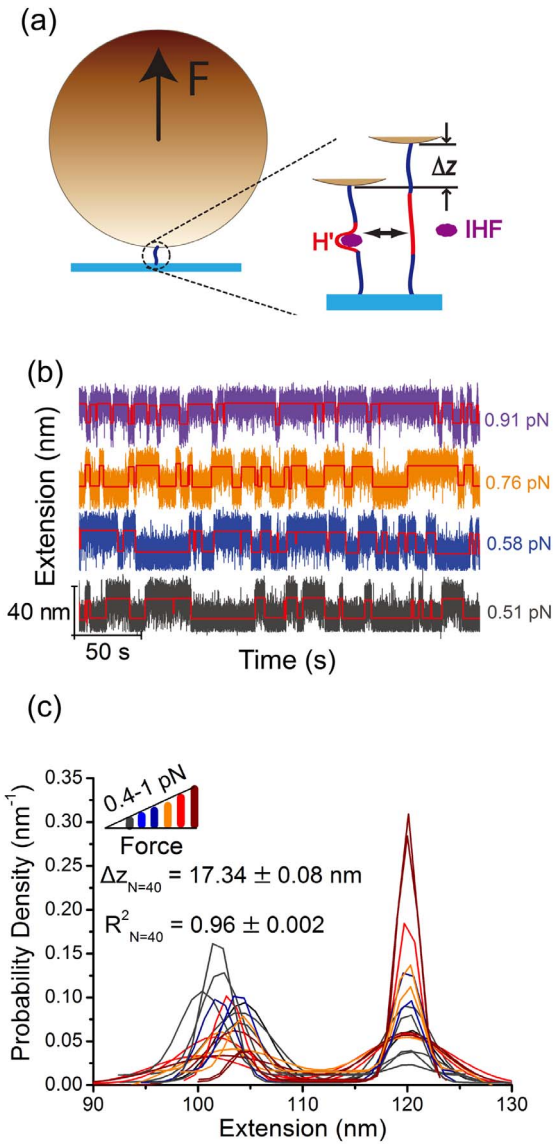

Figure 1 | Two conformational states of DNA-IHF complex. (a). A sketch of the principle of the measurement. The H′ DNA bending by IHF binding reduces the DNA extension, which is detected by the resulting change of the height of the bead. (b). Dynamic fluctuations between two extensions in 10 nM IHF, 50 mM KCl, 2.5 mM $MgCl_2$, 10 mM Tris (pH 7.4), and 21°C at different forces (0.5–1 pN) indicated by different colors. The red line represents extension steps detected a noise-beating step-finding algorithm (SM-Text "Noise-beating step-finding algorithm"). (c). The probability densities of the two extension states, which were produced by the double Gaussian fitting of the normalized histogram of smoothed data at different forces (0.4–1 pN, represented by different colors) using a bin size of 1 nm. A statistics of 40 distributions gave a step size of 17.34 ± 0.08 (mean ± s.d.) nm and R^2 = 0.96 ± 0.022 (mean ± s.d.). Note, only 13 fitting lines from 5 DNA molecules were shown in figure for clarity.

$$P_{\text{bent}} = \frac{\text{Exp}[(\Delta G - \Delta z \times f)/k_B T]}{1 + \text{Exp}[(\Delta G - \Delta z \times f)/k_B T]} \quad (1)$$

where ΔG is the Gibbs free energy difference between the unbent and bent DNA conformations in the absence of force, Δz is the step size of two-state fluctuation, and f is the force applied to the DNA. While ΔG describes the stability of the interaction between IHF and H′, it depends on the protein concentration C. The intrinsic stability of the interaction is described by the dissociation constant K_d, which

is a concentration independent quantity and is related to ΔG through: $K_d = C \times \mathrm{Exp}(-\Delta G/k_BT)$. A lower value of K_d indicates a stronger interaction. Substituting ΔG with K_d and C, Eq. (1) becomes:

$$P_{\mathrm{bent}} = \frac{(C/K_d) \times \mathrm{Exp}(-\Delta z \times f/k_BT)}{1 + (C/K_d) \times \mathrm{Exp}(-\Delta z \times f/k_BT)} \qquad (2)$$

This equation explicitly expresses the dependence of P_{bent} on both force and protein concentration, as well as the dissociation constant of the specific interaction between H′ and IHF. In our experiments, C and f were given as experimental parameters and the resulting P_{bent} and Δz were measured; therefore K_d is the only free parameter that can be determined by fitting the experimental data to Eq. (2). As the fluctuation step size Δz is narrowly distributed around its average, for simplicity Δz was set to be a constant at its average value (17.34 nm) in our fitting.

Fig. 2 shows the fitting at two different temperatures 21 ± 1°C (dark gray) and 31 ± 1°C (red) in 50 mM KCl, which yielded the average values of K_d associated with fitting standard errors of 0.44 ± 0.06 nM and 1.54 ± 0.08 nM, respectively, using data from multiple (≥3) independent experiments under respective temperatures. The results showed that the bent DNA state in an IHF-H′ complex became less stable as temperature increased.

At a higher salt concentration of 200 mM KCl containing 2.5 mM $MgCl_2$, two-state fluctuation was not observed at 21°C, indicating that the unbent DNA state dominated in the force range in the presence of 10 nM IHF (Fig. S4). We reasoned that this could be due to reduced binding affinity at higher salt concentration; therefore, we investigated IHF binding at higher IHF concentrations of 100, 500 and 1000 nM, where two-state fluctuations were observed

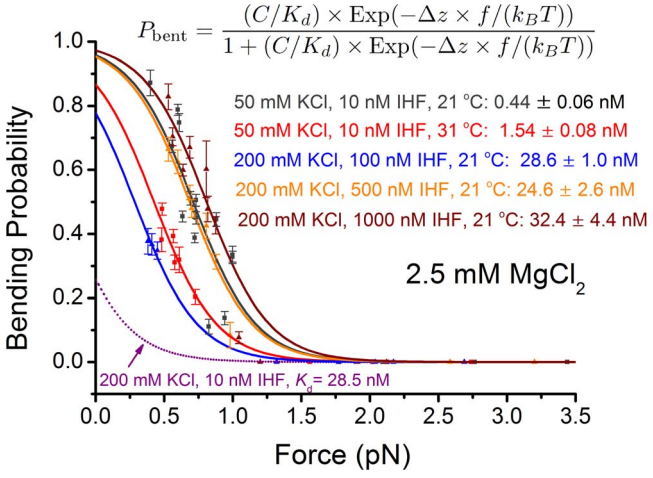

Figure 2 | The effects of temperature, KCl concentration and IHF concentration on H′ DNA bending. The bending probability as a function of force in 2.5 mM $MgCl_2$, 10 mM Tris (pH 7.4), at 10 nM IHF, 50 mM KCl, 21° (dark gray symbols), 10 nM IHF, 50 mM KCl, 31°C (red symbols), 100 nM IHF, 200 mM KCl, 21°C (blue symbols), 500 nM IHF, 200 mM KCl, 21°C (orange symbols), and 1000 nM IHF, 200 mM KCl, 21°C (wine symbols). Data for each solution condition were obtained from multiple (≥3) independent DNA molecules. Error bars for each data points (symbols) were standard deviations from multiple (≥3) repeating measurements for the same DNA molecules. The bending probabilities were calculated by the relative area of the two species in the bimodal extension distribution. Under each solution condition, data obtained were fitted by the two-state model (Eq.(2)) to obtain K_d and the standard error of K_d (fitting error), which are indicated in figure panels by corresponding colors. The goodness of the fitting (R^2) are 0.84, 0.98, 0.94, 0.93, 0.99, respectively. The purple dot line is the theoretical calculation of the bending probability in 10 nM IHF, 200 mM KCl, 2.5 mM $MgCl_2$, based on the two-state model with an averaged K_d = 28.5 nM.

(Fig. S4). Fig. 2 shows the resulting force dependent bending probabilities (symbols), the corresponding two-state theoretical fitting based on Eq. (2) (lines), indicated by blue, orange and wine colors, respectively. K_d estimated from the three different IHF concentrations at 200 mM KCl were overall consistent with each other, with a value of 28.5 ± 3.9 nM (mean ± s.d.). Based on the K_d estimated at 200 mM KCl, the bending probability at 10 nM IHF in the force range of 0.5–1 pN was predicted to be lower than 5%, which explained why we did not observe two-state fluctuations in 10 nM IHF at 200 mM KCl.

Here we note that the salt dependence of IHF binding to DNA is rather complex, related to release of counterions when IHF initially weakly binds to DNA and further release of counterions which is countered by simultaneous release of water molecules in the following tightly bending process. As a result, the first step is sensitive to KCl concentration while the second is less sensitive[28,29]. Increasing KCl concentration will reduce the first step of binding; therefore higher IHF concentration is needed to observe the two-state IHF dependent fluctuation in our experiments.

The lower extension state can be explained by bending of the H′ DNA sequence associated with an IHF. However, the longer extension state may have two alternative explanations: a DNA without an IHF bound at H′, or an IHF-H′ complex in a non-bent, intermediate state. The values of K_d of ~1 nM for 50 mM KCl, 2.5 mM $MgCl_2$, and that of ~28 nM for 200 mM KCl, 2.5 mM $MgCl_2$ determined in our experiments agree with values determined in previous bulk experiments[4,11], suggesting that the two-state fluctuations in our experiments are likely dominated by dissociation and association of IHF to the H′ sequence of DNA.

The specific structure of IHF-H′ complex was solved by X-ray crystallization, which indicated that the 34 bp H′ DNA is bent over the surface of an IHF hetero-dimer by an angle ~160°[5]. The H′ bending angle by IHF was also estimated by AFM imaging to be >120°[12–14]. Both of these methods determined the angles based on static conformations of the IHF-H′ complex. The DNA bending angle can also be estimated from our dynamic two-state extension fluctuation data under constant forces in solution. DNA can be described as a semi-flexible worm-like-chain (WLC) polymer model with a DNA bending persistence length of A ~ 50 nm[30,31]. In the WLC model, a DNA of contour length of L can be modeled as a chain of N segments, each with a segment length of $b \ll A$. The bending energy cost in units of k_BT of one DNA segment is described by: $E_i(\hat{\mathbf{t}}_i, \hat{\mathbf{t}}_{i+1}) = \frac{1}{2}\frac{A}{b}(\hat{\mathbf{t}}_i - \hat{\mathbf{t}}_{i+1})^2$, where i denotes the i_{th} vertex connecting the i_{th} and $(i+1)_{\mathrm{th}}$ segments, and $\hat{\mathbf{t}}_i$ is the tangent vector of the i_{th} segment. The total bending energy is the sum of all the bending energies carried by each vertex: $E = \sum_{i=1}^{N-1} E_i(\hat{\mathbf{t}}_i, \hat{\mathbf{t}}_{i+1})$.

In our experiments, the 445 bp DNA contains one specific H′ site near the middle of the DNA that is subject to binding and unbinding of IHF. To estimate the level of overall extension reduction of the DNA tether under constant forces when an IHF is associated to the H′ site, we discretized our DNA by a segment length of b = 1 nm. The H′ site associated with an IHF was modeled as a point-like kinked site placed at the middle of the DNA, which has a preferred bending angle described by a parameter γ: $\theta = \cos^{-1}\gamma$. The bending energy of this site is therefore modified to be: $E_{\mathrm{kink}}(\hat{\mathbf{t}}, \hat{\mathbf{t}}') = \frac{a}{2}(\hat{\mathbf{t}} \cdot \hat{\mathbf{t}}' - \gamma)^2$[27,32,33] where the $\hat{\mathbf{t}}$ and $\hat{\mathbf{t}}'$ are the tangent vectors of the two successive segments involved in the kink; the dimensionless parameter a describes the deformability of the kinked site, which was chosen to be a large number to ensure a rigid kink (a = 50 nm was chosen in our calculation for Figure 3, but note the extension reduction versus force profiles are insensitive to the value of a as shown in Figure S6). The rest of DNA remained in the naked DNA state and follow WLC model.

The force-extension curves of the DNA tether with various values of preferred bending angle θ at the kinked H′ site were calculated using a previously developed transfer-matrix method[27,32,33]. The curves shift downward as θ increases (Fig. S6a), leading to an extension reduction Δz compared to DNA without the kink defect. Fig. 3 shows Δz versus force at several DNA bending angles in the range of 90–180°, converted from γ in the range of $[-1,0]$ by $\theta = \cos^{-1}\gamma$. In our experiment, the force range where the two-state fluctuations were observed was around 0.5–1 pN, which was associated with extension fluctuation step sizes (i.e, Δz) of ~17.34 nm. By comparison with the theoretical prediction in Fig. 3, these values corresponded to predictions with a preferred DNA bending angle of 140–180°. The bending angle θ was also independently estimated by an approximate analytical formula derived by Kulić *et al*[34].: $\Delta z = 4\left(1-\cos\left(\frac{\theta}{4}\right)\right)\sqrt{\frac{k_BTA}{f}}$, which is valid for forces $\gg \frac{k_BT}{A} \sim 0.08$ pN where the entropic DNA conformational fluctuation is suppressed. This analytical formula also gave similar estimated bending angle to that observed in our experimental force range (Fig. S6). Overall, the bending angle range estimated from our dynamic fluctuations is consistent with the large H′ DNA bending observed from previous X-ray crystallization and AFM imaging experiments[5,12–14].

Discussion

In the present study, we showed that specific DNA-protein interactions can be probed by stretching short DNA molecules. Previous single-DNA stretching studies of DNA-protein interactions were usually restricted to DNA length of a few microns[35], while some recent studies have pushed the length limit to ~700 nm (~2000 bp)[36,37]. It was shown that the protein density on DNA must be high enough in order to see a detectable effect. As an example, for DNA bending by 90°, the spacing between two adjacent bends needs to be below 100 nm in order to see an obvious shift in force-extension curves[27]. The low signal-to-noise ratio resulted from large conformational fluctuation of long DNA has made it difficult to detect protein binding at a low protein density on DNA[27]. As a result, those previous studies were mainly restricted to non-specific DNA-protein interactions at rather high protein concentrations to ensure sufficient binding density for detection, including studies on bacterial IHF[16,38], H-NS[39–41], HU[42,43], archaeal Alba, Cren7 and Su17[44,45], and eukaryotic HMGB[46].

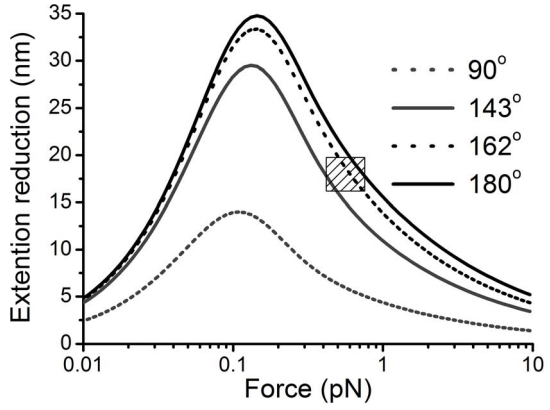

Figure 3 | Theoretical prediction of the effect of bending angle and force on the extension of short DNA. The extension reduction (Δz) of a DNA with a contour length of 150 nm induced by a kink placed at the middle as a function of force and bending angles $\theta = 90°$ (gray dotted line), 143° (gray solid line), 162° (black dotted line), 180° (black solid line). The shadow area represents the rough force range and Δz range measured in experiments.

Compared to previous biochemistry methods to probe specific DNA-protein interactions[4,11,17,18,22], stretching short DNA has unique advantages to directly probe real time distortion of DNA by binding of a single protein. Compared to fluorescence based single-molecule method such as FRET[19], single-DNA stretching does not require fluorescence labeling and is able to monitor protein-DNA interaction over much longer time scales and distance range. Compared to the tethered particle motion that also probes the dynamics of DNA conformational changes by protein binding[21], single-DNA stretching provides additional information of the potential regulatory role of force applied to DNA. Thus, our results demonstrate that stretching short DNA provides a powerful experimental approach for studies of specific DNA-protein interactions under force, which is complimentary to previously developed biochemistry and biophysical methods.

The intracellular concentration of IHF (12–55 μM[15]) is much higher than the concentration needed for site-specific functions; therefore non-specific binding of IHF also occurs. When IHF binds to DNA non-specifically, it occupies less number of DNA base pairs (~10 bp)[17], and causes a much less DNA bending angle (<30°) at the binding sites[16]. This is in sharp contrast to specific binding of IHF to the H′ sequence that occupies 34 bp DNA and causes a bending angle of >120°[5,12–14].

Despite that *in vivo* the complicated protein-DNA interactions may significantly differ from *in vitro* studies in kinetics and stability, our results of the ultra sensitivity of the IHF-H′ to force provided important insights to the potential physiological role of force in regulating the activities of transcription factors. The nucleoid is known attached to the cell wall[47], which may lead to building up tension in DNA due to DNA compaction by nucleoid associated proteins. Forces in picoNewton range can be expected based on k_BT interaction energy between proteins and DNA with nm scale of interaction distance. Force on DNA can also be produced during transcription, as RNA polymerases are known able to generate >20 pN forces[6]. Therefore, our finding that IHF-H′ interaction is sensitive to sub-picoNewton forces is likely physiologically relevant.

We showed that the binding and unbinding of IHF to its specific site can sense small forces <1 pN, and can be fine tuned by sub pN force changes. At zero force, P_{bent} is larger than 95% at 50 mM KCl, 2.5 mM $MgCl_2$ and 21°C (Fig. 2), consistent with the previous reported stable IHF-H′ complex in the absence of force[4,11,12,21]. Such ultra force sensitivity of the IHF-H′ interaction relies on a large dimensional change of DNA by protein-induced DNA bending. The ~17 nm step size resulted from large DNA conformational change observed in our experiments implies that a small force around $\frac{k_BT}{17\text{ nm}} \sim 0.2$ pN can perturb the IHF-H′ interaction, which is close to the force range observed in our experiments. As the functions of many site specific transcription factors rely on sharp DNA bending[48,49] or DNA looping[50,51] that cause large conformational change of DNA, our results suggest that force on DNA may sensitively regulate the functions of a broad class of site specific DNA binding transcription factors.

These results also demonstrated that the level of DNA distortion at the specific site bound with a protein can be estimated from the dynamic extension fluctuation between protein-bound and protein-unbound states based on DNA polymer physics. In the case of IHF-H′ interaction investigated in our work, the difference of the DNA bending angle (140–180°) estimated from our data and that determined in X-ray crystallization (~160°)[5] is within 15%. A unique advantage of the approach of short DNA stretching to determine protein induced DNA distortion is that it is not limited to any specific solution conditions such as temperature, salt, pH, and protein concentrations.

Previously, IHF binding to a short DNA tether of 76 bp containing the H′ sequence was studied by monitoring the displacement of a bead attached to one end of DNA from a cover glass in the presence of 100 nM IHF in 1xPBS[52]. In that experiment, longitude fluctuation of the bead was recorded and used to re-construct the potential. Force was calculated by the gradient of the potential, which depended on the distance between the bead and the cover glass surface and therefore was not constant during DNA extension fluctuation. An ~8 nm extension change between the bent and unbent DNA conformation states was reported[52], which was ~ ½ of that in our observation. We propose that this difference might be caused by different level of DNA wrapping on IHF. Most of DNA bending by IHF heterodimer mainly occurs at two large kinked steps where the minor groove of DNA at each location is intercalated by one proline residue at the tip of the β-ribbon arm from each IHF subunit[5]. In the work by Dixit *et al.*, tension on DNA increased rapidly during the wrapping process[52], which might prevent complete wrapping of DNA on IHF, i.e., possibly only one location is intercalated by a proline residue from one of the IHF subunits. This would lead to a smaller bending angle and explain why they observed a smaller extension difference between naked and wrapped DNA than we observed. In contrast, full DNA wrapping might occur in our experiments, as during wrapping a constant force is maintained. Our current study has further improved from that pioneering study by applying accurately controlled constant forces to DNA, which allowed us to extract more comprehensive information of the interaction between IHF and H′ DNA, such as the dissociation constant K_d and the bending angle of the IHF-H′ complex.

Several possible intermediate conformational states have been suggested previously[11,19]. Using a noise-beating algorithm, some minority transitions associated with <10 nm steps were detected, which is consistent with the presence of such intermediate states (See Figure S7). Future work will be directed to improve the spatial resolution of our instrument as well as combine with single-molecule FRET technology to better resolve those possible intermediate states and their stabilities.

Methods

An improved magnetic tweezers with a spatial resolution of ~2 nm and a sampling rate of 100 Hz which is capable of stretching both short DNA and protein[23,53–55] was used in the experiments. Details of DNA construct and protein, magnetic tweezers measurement, temperature control, data analysis methods and supplementary figures can be found in the Supplementary information.

1. Ishihama, A. Prokaryotic genome regulation: multifactor promoters, multitarget regulators and hierarchic networks. *FEMS Microbiol. Rev.* **34**, 628–45 (2010).
2. Ishihama, A. Functional modulation of Escherichia coli RNA polymerase. *Annu. Rev. Microbiol.* **54**, 499–518 (2000).
3. Nash, H. A. & Robertson, C. A. Purification and properties of the Escherichia coli protein factor required for lambda integrative recombination. *J. Biol. Chem.* **256**, 9246–53 (1981).
4. Yang, S. W. & Nash, H. A. Comparison of protein binding to DNA in vivo and in vitro: defining an effective intracellular target. *EMBO J.* **14**, 6292–300 (1995).
5. Rice, P. A., Yang, S., Mizuuchi, K. & Nash, H. A. Crystal structure of an IHF-DNA complex: a protein-induced DNA U-turn. *Cell* **87**, 1295–306 (1996).
6. Wang, M. D. *et al.* Force and velocity measured for single molecules of RNA polymerase. *Science* **282**, 902–7 (1998).
7. Wuite, G. J., Smith, S. B., Young, M., Keller, D. & Bustamante, C. Single-molecule studies of the effect of template tension on T7 DNA polymerase activity. *Nature* **404**, 103–6 (2000).
8. Arfin, S. M. *et al.* Global gene expression profiling in Escherichia coli K12 - The effects of integration host factor. *J. Biol. Chem.* **275**, 29672–29684 (2000).
9. Mangan, M. W. *et al.* The integration host factor (IHF) integrates stationary-phase and virulence gene expression in Salmonella enterica serovar Typhimurium. *Mol. Microbiol.* **59**, 1831–1847 (2006).
10. Luijsterburg, M. S., Noom, M. C., Wuite, G. J. L. & Dame, R. T. The architectural role of nucleoid-associated proteins in the organization of bacterial chromatin: A molecular perspective. *J. Struct. Biol.* **156**, 262–272 (2006).
11. Sugimura, S. & Crothers, D. M. Stepwise binding and bending of DNA by Escherichia coli integration host factor. *Proc. Natl. Acad. Sci. U.S.A.* **103**, 18510–18514 (2006).
12. Bao, Q. Y. *et al.* A divalent metal-mediated switch controlling protein-induced DNA bending. *J. Mol. Biol.* **367**, 731–740 (2007).
13. Seong, G. H., Kobatake, E., Miura, K., Nakazawa, A. & Aizawa, M. Direct atomic force microscopy visualization of integration host factor-induced DNA bending structure of the promoter regulatory region on the Pseudomonas TOL plasmid. *Biochem. Biophys. Res. Commun.* **291**, 361–6 (2002).
14. Dame, R. T. *et al.* Analysis of scanning force microscopy images of protein-induced DNA bending using simulations. *Nucleic Acids Res.* **33**, e68 (2005).
15. Ali Azam, T., Iwata, A., Nishimura, A., Ueda, S. & Ishihama, A. Growth phase-dependent variation in protein composition of the Escherichia coli nucleoid. *J. Bacteriol.* **181**, 6361–70 (1999).
16. Lin, J., Chen, H., Droge, P. & Yan, J. Physical Organization of DNA by Multiple Non-Specific DNA-Binding Modes of Integration Host Factor (IHF). *Plos One* **7**, e49885 (2012).
17. Holbrook, J. A., Tsodikov, O. V., Saecker, R. M. & Record, M. T. Specific and non-specific interactions of integration host factor with DNA: Thermodynamic evidence for disruption of multiple IHF surface salt-bridges coupled to DNA binding. *J. Mol. Biol.* **310**, 379–401 (2001).
18. Craig, N. L. & Nash, H. A. Escherichia-Coli Integration Host Factor Binds to Specific Sites in DNA. *Cell* **39**, 707–716 (1984).
19. Kuznetsov, S. V., Sugimura, S., Vivas, P., Crothers, D. M. & Ansari, A. Direct observation of DNA bending/unbending kinetics in complex with. DNA-bending protein IHF. *Proc. Natl. Acad. Sci. U.S.A.* **103**, 18515–18520 (2006).
20. Lorenz, M., Hillisch, A., Goodman, S. D. & Diekmann, S. Global structure similarities of intact and nicked DNA complexed with IHF measured in solution by fluorescence resonance energy transfer. *Nucleic Acids Res.* **27**, 4619–25 (1999).
21. Zurla, C. *et al.* Integration host factor alters LacI-induced DNA looping. *Biophys. Chem.* **128**, 245–252 (2007).
22. Vivas, P., Velmurugu, Y., Kuznetsov, S. V., Rice, P. A. & Ansari, A. Mapping the Transition State for DNA Bending by IHF. *J. Mol. Biol.* **418**, 300–315 (2012).
23. Chen, H. *et al.* Improved High-Force Magnetic Tweezers for Stretching and Refolding of Proteins and Short DNA. *Biophys. J.* **100**, 517–523 (2011).
24. Lusk, J. E., Williams, R. J. & Kennedy, E. P. Magnesium and the growth of Escherichia coli. *J. Biol. Chem.* **243**, 2618–24 (1968).
25. Cui, Y. B., Petrushenko, Z. M. & Rybenkov, V. V. MukB acts as a macromolecular clamp in DNA condensation. *Nat. Struct. Mol. Biol.* **15**, 411–418 (2008).
26. Craig, N. L. & Nash, H. A. E. coli integration host factor binds to specific sites in DNA. *Cell* **39**, 707–16 (1984).
27. Yan, J. & Marko, J. F. Effects of DNA-distorting proteins on DNA elastic response. *Phys. Rev. E* **68**, 011905 (2003).
28. Vivas, P., Velmurugu, Y., Kuznetsov, S. V., Rice, P. A. & Ansari, A. Global analysis of ion dependence unveils hidden steps in DNA binding and bending by integration host factor. *J. Chem. Phys.* **139**, 121927 (2013).
29. Vivas, P., Kuznetsov, S. V. & Ansari, A. New insights into the transition pathway from nonspecific to specific complex of DNA with Escherichia coli integration host factor. *J. Phys. Chem. B* **112**, 5997–6007 (2008).
30. Bustamante, C., Marko, J. F., Siggia, E. D. & Smith, S. Entropic Elasticity of Lambda-Phage DNA. *Science* **265**, 1599–1600 (1994).
31. Marko, J. F. & Siggia, E. D. Stretching DNA. *Macromolecules* **28**, 8759–8770 (1995).
32. Chen, H. & Yan, J. Effects of kink and flexible hinge defects on mechanical responses of short double-stranded DNA molecules. *Phys. Rev. E* **77**, 041907 (2008).
33. Yan, J., Kawamura, R. & Marko, J. F. Statistics of loop formation along double helix DNAs. *Phys. Rev. E* **71**, 061905 (2005).
34. Kulic, I. M., Mohrbach, H., Thaokar, R. & Schiessel, H. Equation of state of looped DNA. *Phys. Rev. E* **75**, 011913 (2007).
35. Neuman, K. C. & Nagy, A. Single-molecule force spectroscopy: optical tweezers, magnetic tweezers and atomic force microscopy. *Nat. Methods* **5**, 491–505 (2008).
36. Revyakin, A., Liu, C., Ebright, R. H. & Strick, T. R. Abortive initiation and productive initiation by RNA polymerase involve DNA scrunching. *Science* **314**, 1139–43 (2006).
37. Revyakin, A., Ebright, R. H. & Strick, T. R. Single-molecule DNA nanomanipulation: improved resolution through use of shorter DNA fragments. *Nat. Methods* **2**, 127–38 (2005).
38. Ali, B. M. J. *et al.* Compaction of single DNA molecules induced by binding of integration host factor (IHF). *Proc. Natl. Acad. Sci. U.S.A.* **98**, 10658–10663 (2001).
39. Noom, M. C., Navarre, W. W., Oshima, T., Wuite, G. J. & Dame, R. T. H-NS promotes looped domain formation in the bacterial chromosome. *Curr. Biol.* **17**, R913–4 (2007).
40. Liu, Y. J., Chen, H., Kenney, L. J. & Yan, J. A divalent switch drives H-NS/DNA-binding conformations between stiffening and bridging modes. *Gene Dev.* **24**, 339–344 (2010).
41. Dame, R. T., Noom, M. C. & Wuite, G. J. L. Bacterial chromatin organization by H-NS protein unravelled using dual DNA manipulation. *Nature* **444**, 387–390 (2006).
42. van Noort, J., Verbrugge, S., Goosen, N., Dekker, C. & Dame, R. T. Dual architectural roles of HU: formation of flexible hinges and rigid filaments. *Proc. Natl. Acad. Sci. U.S.A.* **101**, 6969–74 (2004).

43. Xiao, B., Zhang, H., Johnson, R. C. & Marko, J. F. Force-driven unbinding of proteins HU and Fis from DNA quantified using a thermodynamic Maxwell relation. *Nucleic Acids Res.* **39**, 5568–77 (2011).
44. Driessen, R. P. *et al.* Crenarchaeal chromatin proteins Cren7 and Sul7 compact DNA by inducing rigid bends. *Nucleic Acids Res.* **41**, 196–205 (2013).
45. Laurens, N. *et al.* Alba shapes the archaeal genome using a delicate balance of bridging and stiffening the DNA. *Nat. Commun.* **3**, 1328 (2012).
46. McCauley, M. J., Rueter, E. M., Rouzina, I., Maher, L. J., 3rd & Williams, M. C. Single-molecule kinetics reveal microscopic mechanism by which High-Mobility Group B proteins alter DNA flexibility. *Nucleic Acids Res.* **41**, 167–81 (2013).
47. Toro, E. & Shapiro, L. Bacterial Chromosome Organization and Segregation. *Cold Spring Harb. Perspect. Biol.* **2**, a000349 (2010).
48. Browning, D. F., Grainger, D. C. & Busby, S. J. W. Effects of nucleoid-associated proteins on bacterial chromosome structure and gene expression. *Curr. Opin. Microbiol.* **13**, 773–780 (2010).
49. Stavans, J. & Oppenheim, A. DNA-protein interactions and bacterial chromosome architecture. *Phys. Biol.* **3**, R1–10 (2006).
50. Matthews, K. S. DNA Looping. *Microbiol. Rev.* **56**, 123–136 (1992).
51. Finzi, L. & Gelles, J. Measurement of Lactose Repressor-Mediated Loop Formation and Breakdown in Single DNA-Molecules. *Science* **267**, 378–380 (1995).
52. Dixit, S., Singh-Zocchi, M., Hanne, J. & Zocchi, G. Mechanics of binding of a single integration-host-factor protein to DNA. *Phys. Rev. Lett.* **94**, 118101 (2005).
53. Fu, H. X., Le, S. M., Chen, H., Muniyappa, K. & Yan, J. Force and ATP hydrolysis dependent regulation of RecA nucleoprotein filament by single-stranded DNA binding protein. *Nucleic Acids Res.* **41**, 924–932 (2013).
54. Fu, H., Le, S., Muniyappa, K. & Yan, J. Dynamics and Regulation of RecA Polymerization and De-Polymerization on Double-Stranded DNA. *PLoS One* **8**, e66712 (2013).
55. Fu, H. X. *et al.* Transition dynamics and selection of the distinct S-DNA and strand unpeeling modes of double helix overstretching. *Nucleic Acids Res.* **39**, 3473–3481 (2011).

Acknowledgments

This work was supported by the National Research Foundation through the Mechanobiology Institute Singapore [to J.Y.], the Ministry of Education of Singapore under Grant MOE 2013-T2-1-154 [to J.Y.], and the Academic Research Council Singapore [Tier 1 to P.D.].

Author contributions

J.Y. and P.D. conceived the research. S.L. and J.Y. designed the experiments. S.L. and J.L. performed the experiments. S.L., H.C., P.C. and J.Y. did data analysis and interpreted the data. H.C., P.C. and J.L. provided technical support. S.L., P.D. and J.Y. wrote the paper.

Additional information

Supplementary information accompanies this paper at http://www.nature.com/scientificreports

Competing financial interests: The authors declare no competing financial interests.

How to cite this article: Le, S. M. *et al.* Mechanosensing of DNA bending in a single specific protein-DNA complex. *Sci. Rep.* **3**, 3508; DOI:10.1038/srep03508 (2013).